Tight inequalities for nonclassicality of measurement statistics

V. S. Kovtoniuk ¹, E. V. Stolyarov ¹, O. V. Kliushnichenko ¹, and A. A. Semenov ¹, 3, 2

¹Bogolyubov Institute for Theoretical Physics, NAS of Ukraine, Vul. Metrolohichna 14-b, 03143 Kyiv, Ukraine
²Institute of Physics, NAS of Ukraine, Prospect Nauky 46, 03028 Kyiv, Ukraine
³Kyiv Academic University, Blvd. Vernadskogo 36, 03142 Kyiv, Ukraine

In quantum optics, measurement statistics—for example, photocounting statistics—are considered nonclassical if they cannot be reproduced with statistical mixtures of classical radiation fields. We have formulated a necessary and sufficient condition for such nonclassicality. This condition is given by a set of inequalities that tightly bound the convex set of probabilities associated with classical electromagnetic radiation. Analytical forms for full sets and subsets of these inequalities are obtained for important cases of realistic photocounting measurements and unbalanced homodyne detection. As an example, we consider photocounting statistics of phase-squeezed coherent states. Contrary to a common intuition, the analysis developed here reveals distinct nonclassical properties of these statistics that can be experimentally corroborated with minimal resources.

I. INTRODUCTION

The concept of nonclassical states in quantum optics [1–9] is based on the fact that all measurements under the coherent states $|\alpha\rangle$ of a light mode can be explained with no need to quantize the electromagnetic field. Since the density operator $\hat{\rho}$ of any quantum state can be represented as

$$\hat{\rho} = \int_{\mathbb{C}} d^2 \alpha P(\alpha) |\alpha\rangle \langle \alpha|, \qquad (1)$$

where $P(\alpha)$ is the Glauber-Sudarshan P-function [10, 11], the states with $P(\alpha) \geq 0$ can be regarded as classical statistical mixtures of coherent states. The remaining states are considered to be nonclassical.

Since the *P*-function is typically highly singular, its direct tomographic reconstruction is feasible only for specific states [12, 13]. Alternatively, one can use modified versions of the P-function [14–16], direct connections between P-function and other regular phase-space functions [17, 18], nonclassicality measures [19–25], informationally complete measurements based on heterodyne detection [26], etc. Another group of nonclassicality tests involves scenarios with partial information obtained through specific measurements or sets of measurements; see, e.g., Refs. [26–30]. The latter tests provide only sufficient conditions for nonclassicality of quantum states. However, they address a more specific but still crucial issue: can the given measurement statistics be reproduced with a statistical mixture of coherent states?

An example is given by photocounting statistics estimated with photon-number resolving (PNR) detectors. The corresponding archetypal tests are based on the Mandel Q-parameter [31], its higher-order generalization [32], the Klyshko criterion [33], etc. The first two have been adapted [34–36] to a realistic scenario with click detectors [37–44]. Other tests [45, 46] involve unbalanced homodyne detection [47], completing photocounters by device settings. Notable tests using field-quadrature values as measurement outcomes verify quadrature squeezing [48–52] and its generalizations [53, 54]. Nonclassical-

ity tests have also been formulated for sets of quadratures; see, e.g., Ref. [55].

Nonclassicality of measurement statistics implies that the probability distributions $\mathcal{P}(A|a)$ to obtain the value A under a measurement with the setting a cannot be expressed as a convex combination of the probability distributions $\Pi(A|a;\alpha) = \langle \alpha | \hat{\Pi}(A|a) | \alpha \rangle$ for the coherent states $|\alpha\rangle$. Here $\hat{\Pi}(A|a)$ is an element of the positive operator-valued measure (POVM), corresponding to the measurement outcome A with the setting a. If A is the number of photons and no detector settings are involved, this aligns with nonclassicality of photon-number statistics in Ref. [56]. Our approach extends this concept to encompass arbitrary observables and device settings.

Drawing upon the deep mathematical similarity between nonclassicality of measurement statistics and Bell nonlocality [57], inequalities have been derived to test the former [26, 58]; see also Ref. [28] and Appendix A. The probability distributions $\mathcal{P}(A|a)$, referred to as behavior [59], are nonclassical iff there exists a function $\lambda(A,a)$ that the inequality

$$\sum_{a,A} \mathcal{P}(A|a)\lambda(A,a) \le \sup_{\alpha \in \mathbb{C}} \sum_{a,A} \Pi(A|a;\alpha)\lambda(A,a) \qquad (2)$$

is violated. The left-hand side of this inequality can be estimated from the measured data, facilitating practical implementation of the test. On the right-hand side the supremum over the coherent amplitude α in the whole complex plane $\mathbb C$ is taken.

Inequality (2) implies that the sum of expectation values of the test-function $\lambda(A,a)$ over all settings a for the classical measurement statistics does not exceed the same sum of its expectation values for all coherent states $|\alpha\rangle$; see Appendix A for details. This inequality has a structure similar to the representation of standard Bell inequalities in Refs. [26, 58]. The latter test Bell nonlocality and differ from Bell-like inequalities (2), which test nonclassicality of measurement statistics, by two points. First, standard Bell inequalities involve at least two spatially-separated parties. Second, their right-hand side involves the incidence matrix [60] instead of $\Pi(A|a;\alpha)$.

Finding the optimal test-function $\lambda(A,a)$ in inequality (2) can be a challenging problem. In this paper, we find that, like it is concluded in studies of Bell nonlocality [57], the amount of these inequalities can be reduced to tightly bound the convex set of classical behaviors. Thus, the problem of finding the optimal $\lambda(A,a)$ is drastically simplified to finding violations among tight inequalities.

In particular, our technique enables one to verify nonclassicality of photocounting statistics for phase-squeezed coherent states using minimal experimental resources. This verification also extends to the case of on-off detectors in the context of unbalanced homodyne detection. The obtained result contradicts the intuitive expectation based on positive excess noise for photocounting measurements with such states [6], implying the positive Mandel Q-parameter.

The rest of the paper is organized as follows. In Sec. II we give a rigorous mathematical definition for tight Bell-like inequalities and adapt a statement from convex analysis that serves as a tool to derive them. Tight Bell-like inequalities for photocounting measurements are considered in Sec. III. In Sec. IV these inequalities are derived for unbalanced homodyne detection. A summary and concluding remarks are given in Sec. V.

II. TIGHT BELL-LIKE INEQUALITIES

We start by introducing a rigorous mathematical definition of tight inequalities. In this context, we closely align with the analogy to standard Bell inequalities, testing Bell nonlocality rather than nonclassicality of measurement statistics. In both scenarios, tight (facet) inequalities represent a necessary and sufficient condition for a behavior to be expressed as a convex combination of other behaviors from a given set. These behaviors are deterministic and classical for Bell nonlocality and nonclassicality of measurement statistics, respectively. As described in Sec. II B 2 of Ref. [57], tight inequalities can be defined as follows.

Definition 1. Let Λ be a set of test functions $\lambda(A, a)$. We say that they produce tight Bell-like inequalities if

- (i) for any $\lambda(A, a) \notin \Lambda$, the corresponding inequality follows from Bell-like inequalities with test functions from Λ ;
- (ii) no inequality with $\lambda(A, a) \in \Lambda$ can be inferred from the other tight Bell-like inequalities.

Alongside the introduced notations for the behavior and test function, we will utilize their vector forms denoted as \mathcal{P} and λ , respectively. These vectors contain all values of P(A|a) and $\lambda(A,a)$. The dimensionality of these vectors can be reduced by the number of device settings due to the normalization condition,

$$\sum_{A} \mathcal{P}(A|a) = 1,\tag{3}$$

for behaviors. Indeed, this equation implies that one of the probabilities $\mathcal{P}(A|a)$ can be expressed in terms of the rest for each a. Substituting it into inequality (2) results in a similar inequality with a redefined test-function $\lambda(A,a)$. Consequently, the inequality (2) can be rewritten as

$$\mathcal{P} \cdot \lambda \le \sup_{\alpha \in \mathbb{C}} \Pi(\alpha) \cdot \lambda, \tag{4}$$

where $\Pi(\alpha)$ represents the behavior of the corresponding coherent state.

The standard methods of convex analysis (see, e.g., Refs. [61, 62]) yield a statement that serves as a practical tool for constructing tight Bell-like inequalities. Prior to introducing this statement, let us recall the concept of closed convex cones and their extreme rays. A closed set L of vectors is a closed convex cone if for any $\lambda_1, \lambda_2 \in L$ the conic combination $C_1\lambda_1 + C_2\lambda_2 \in L$, where $C_{1,2} \geq 0$. The extreme rays of L, denoted as $\operatorname{Ext}[L]$, comprise a continuous, discrete, or hybrid set of vectors λ_i such that any $\lambda \in L$ can be expressed as a conic combination of these vectors, i.e., $\lambda = \sum_i C_i \lambda_i$, where $C_i \geq 0$, and sum is replaced by integral for continuous i. Additionally, no vector $\lambda_k \in \operatorname{Ext}[L]$ can be represented as a conic combination of other vectors in this set.

Statement 1. Let us consider the closed convex cones defined by

$$L(\alpha) = \left\{ \boldsymbol{\lambda} \middle| \underset{\alpha' \in \mathbb{C}_{\infty}}{\arg \max} \boldsymbol{\Pi}(\alpha') \cdot \boldsymbol{\lambda} = \alpha \right\}.$$
 (5)

The set Λ , producing tight Bell-like inequalities, can be obtained as

$$\Lambda = \bigcup_{\alpha \in \mathbb{C}_{\infty}} \operatorname{Ext} \left[L(\alpha) \right]. \tag{6}$$

Proof details of this statement, adapted to the considered case, can be found in Appendix B. The behaviors of coherent states in the space of behaviors form a two-or one-dimensional manifold $\mathcal{P} = \Pi(\alpha)$. According to Statement 1, the vectors λ for each value of α can be obtained from the condition $\nabla_{\alpha}[\Pi(\alpha) \cdot \lambda] = \mathbf{0}$, which indicates that they are normal vectors to this manifold at each point parametrized by α . However, in certain cases (such as extreme values of α), the maximum of $\Pi(\alpha) \cdot \lambda$ may not correspond to the zero gradient vector of this relation, and consequently the vectors λ cannot be considered normal to the mentioned manifold. In essence, the process of deriving tight Bell-like inequalities is equivalent to constructing convex sets for all points on this manifold.

III. PHOTOCOUNTING MEASUREMENTS

Let us consider photocounting measurements. In this case, the measurement outcomes correspond to the values

 $A=n\in 0,\ldots,N$, where N is the maximum possible number of detection clicks or the cutoff for the number of photons. Since the photocounter has only one setting, the dimensionality of the behavior is N. For the PNR detectors, the behavior of coherent states is given by (see Ref. [3, 63])

$$\Pi(n|\alpha) = \frac{|\alpha|^{2n}}{n!} \exp\left(-|\alpha|^2\right),\tag{7}$$

where $n = 0 \dots N - 1$.

A more realistic scenario involves click detectors, which utilize spatial [37–40] or temporal [41–43] splitting of the light beam into several modes, followed by separate detection of each mode by on-off detectors. The corresponding behaviors of coherent states read (see Ref. [44])

$$\Pi(n|\alpha) = \binom{N}{n} e^{-(N-n)|\alpha|^2/N} \left(1 - e^{-|\alpha|^2/N}\right)^n, \quad (8)$$

where N represents the number of on-off detectors. In both cases, we consider the detection efficiency to be unity and attribute the detection losses to the quantum states.

Other realistic scenarios of photocounting measurements can also be considered, such as photocounting with avalanche photodiodes affected by dead time and afterpulses [64], or superconducting nanowire single-photon detectors [65]. Since all these cases correspond to phase-insensitive measurements, the behaviors of coherent states, denoted as $\Pi(\alpha)$, do not depend on the phase of α . To conveniently parameterize them, we introduce the parameter $t=e^{-|\alpha|^2/N}\in[0,1]$. Evidently, the behaviors of coherent states form an open curve in an N-dimensional space, with the beginning and end points corresponding to t=0 and t=1, respectively. For the sake of brevity, we also adopt the symbol $\Pi(t)$ to represent the dependence of behaviors of coherent states in photocounting measurements on the parameter t.

A. Photocounting with N=2

Since the binary outcomes (N=1) in photocounting measurements are not capable for testing nonclassicality [26, 34], we start our consideration with the simplest nontrivial case of N=2, corresponding to two-dimensional behaviors. Evidently, the behaviors of coherent states are represented in this case by the open curve in a two-dimensional space, $\mathcal{P}(0)=\Pi(0|t)$ and $\mathcal{P}(1)=\Pi(1|t)$. This curve can also be defined via an explicit equation as $\mathcal{P}(1)=\Pi_1(\mathcal{P}(0))$. We restrict our consideration with detectors, which (i) $\Pi(0|t=0)=\Pi(1|t=0)=0$, i.e., the detector is saturated at $|\alpha|^2 \to +\infty$; (ii) $\Pi(0|t=1)=1$, $\Pi(1|t=1)=0$, i.e., no dark counts are present; (iii) the second derivative of $\Pi_1(x)$ obeys $\Pi_1''(x) \leq 0$.

The direct application of Statement 1 in this case implies finding $\lambda(t)$ from the equation $\dot{\mathbf{\Pi}}(t) \cdot \lambda(t) = 0$ for

each $t \in (0, 1)$. The corresponding extreme ray consists of a single vector normal to the curve $\mathcal{P} = \Pi(t)$,

$$\lambda(t) = \left(-\dot{\Pi}(1|t) \ \dot{\Pi}(0|t)\right). \tag{9}$$

The sets Ext [L(t=0)] and Ext [L(t=1)] comprise the vectors $\lambda(0)$ and $\lambda(1)$, respectively, and the vector (0 - 1). The latter results in a trivial inequality for the nonnegativity of $\mathcal{P}(1)$.

Therefore, the set of tight Bell-like inequalities for the considered case is given by

$$\mathbf{P} \cdot \lambda(t) \le \mathbf{\Pi}(t) \cdot \lambda(t). \tag{10}$$

This set of linear inequalities can be combined into a single nonlinear inequality as

$$\mathcal{P}(1) \le \Pi_1(\mathcal{P}(0)). \tag{11}$$

In the case of PNR detectors, cf. Eq. (7), this leads to inequality $\mathcal{P}(1) \leq -\mathcal{P}(0) \ln \mathcal{P}(0)$ derived with a different technique in Ref. [66]. In the case of click detectors, cf. Eq. (8), inequality (11) reduces to the form

$$[2\mathcal{P}(0) + \mathcal{P}(1)]^2 - 4\mathcal{P}(0) \le 0. \tag{12}$$

Violation of this inequality is a necessary and sufficient condition for nonclassicality of the behavior \mathcal{P} and a sufficient condition for nonclassicality of the corresponding quantum state.

We demonstrate the applicability of this method with the statistics of the attenuated Fock state $|n\rangle$. In this scenario inequality (12) takes the form $(1 - \eta/2)^{2n} \le (1 - \eta)^n$, where $\eta \in]0,1]$ is the efficiency. This inequality is always violated, although for large n the detector is saturated and the violation becomes small.

B. Photocounting with N = 2m + 1, $m \in \mathbb{N}$

The larger number of possible measurement outcomes enables us to verify nonclassicality of photocounting statistics for a broader range of quantum states. We focus on scenarios with N being an odd number. For a set $\boldsymbol{t} = \{t_1, \ldots t_m\}$ of $t_i \in [0,1]$ such that $0 \le t_1 < t_2 < \ldots < t_m \le 1$ and $\tau \in [0,1]$, where $t_i \ne \tau$ for any $i=1\ldots m$, we define the vectors

$$\lambda(t;\tau) = \pm \left(\star \bigwedge_{i=1}^{m} \Delta \Pi(t_i) \wedge \dot{\Pi}(t_i) \right). \tag{13}$$

Here $\Delta \Pi(t_i) = \Pi(t_i) - \Pi(\tau)$ and \star is the Hodge star, see Ref. [67] and Appendix C1. These vectors fulfill the conditions,

$$\mathbf{\Pi}(t_i) \cdot \boldsymbol{\lambda}(t;\tau) = \mathbf{\Pi}(\tau) \cdot \boldsymbol{\lambda}(t;\tau), \tag{14}$$

$$\dot{\mathbf{\Pi}}(t_i) \cdot \boldsymbol{\lambda}(t;\tau) = 0, \tag{15}$$

for $i = 1 \dots m$.

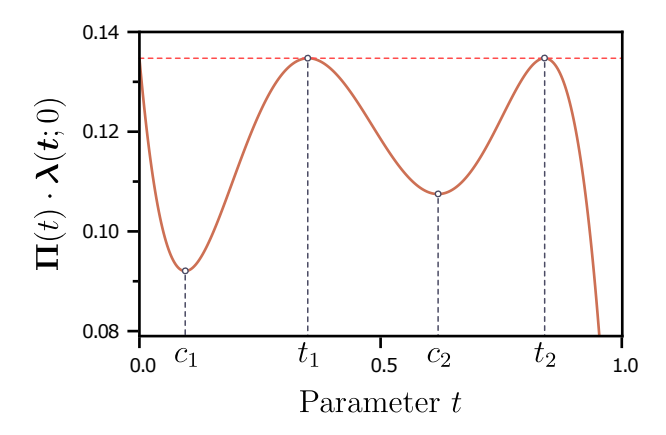


FIG. 1. An example of $\Pi(t) \cdot \lambda(t; \tau = 0)$ as a function of t for click detectors with N = 5 (i.e., m = 2) is shown. The sets of points $0, t_1, t_2$ and c_1, c_2 correspond to global maxima and local minima, respectively.

Let us prove that there exists a class of detectors for which the test functions given by Eq. (13) define tight Bell-like inequalities. Equations (14) and (15) represent a set of 2m linear constraints, which, if not degenerate, define $\lambda(t;\tau)$ given by Eq. (13) up to a constant factor. These equations are also necessary but not sufficient conditions for $\lambda(t;\tau) \in \Lambda$. Indeed, Eq. (15) does not imply that the function $\Pi(t_i) \cdot \lambda(t;\tau)$ does not reach a maximum at the points t_i and even if it did, there would still be no guarantee that it is global. For a wide class of detectors, however, the points t_i and τ are the global maximum of the above function; cf. Fig. 1. This conclusion is the essence of the following statement.

Statement 2. Apart from $t_1, \ldots t_m$, let $\Pi(t) \cdot \lambda(t, \tau)$ have m other critical points at $t \in]0, 1[$. Furthermore, $\ddot{\Pi}(t) \cdot \lambda(t; \tau)$ has 2m-1 zeros at $t \in]0, 1[$. Then one can choose such a sign of $\lambda(t; \tau)$ in Eq. (13), that the global maximum of $\Pi(t) \cdot \lambda(t; \tau)$ is attained for $t = t_i$ and $t = \tau$.

The proof of this statement can be found in Appendix C 2. In Appendix C 3 it is shown that the PNR and click detectors defined by Eqs. (7) and (8), respectively, satisfy the conditions of this statement. Therefore, for each point t we have found a set of test functions λ , such that the $\Pi(t) \cdot \lambda$ reaches the global maximum.

Next we show that every $\lambda(t;\tau)$ defined by Eq. (13) belongs to $\operatorname{Ext}[L(t_k)]$ for every t_k . A similar statement can be proved for $\operatorname{Ext}[L(\tau)]$. Suppose $\lambda(t;\tau) \notin \operatorname{Ext}[L(t_k)]$. Then, there exist such $\lambda_1, \lambda_2 \in L(t_k)$ that $\lambda(t;\tau)$ is their conic combination; cf. Ref. [61] and Appendix C4. In this case it can be shown that they fulfill the above conditions (14) and (15) for $\lambda(t;\tau)$. These conditions represent a non-degenerate system of N linear homogeneous equations for N components of λ . The solutions to this system are given by the colinear vectors. Thus, $\lambda(t;\tau)$ cannot be expanded with two other non-colinear vectors. This means that $\lambda(t;\tau) \in \operatorname{Ext}[L(t_k)]$; cf. Ref. [61] and Appendix C4. This implies that the vectors $\lambda(t;\tau)$, given by Eq. (13), belong to a set of tight Bell-like in-

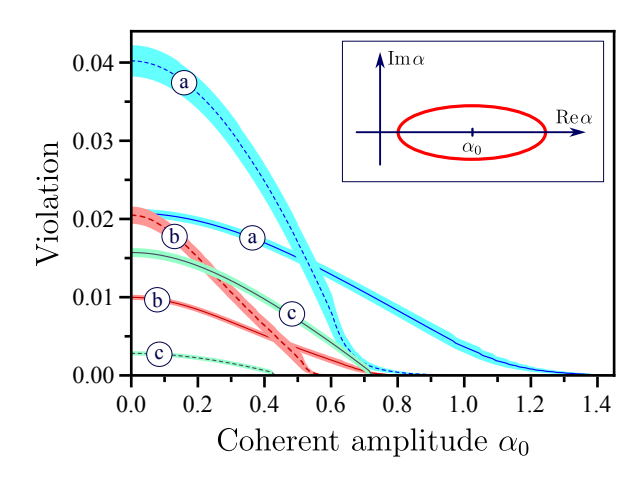


FIG. 2. The maximum violation of the tight Bell-like inequalities (difference of their left- and right-hand sides optimized by parameters t and τ) with the test function given by Eq. (13) for photocounts of phase-squeezed coherent states vs the coherent amplitude α_0 is shown; the Wigner function of such a state is mimicked by its contour line in the inset. The confidence intervals correspond to the standard deviations for estimations of inequality left-side with 10^5 sample events. The solid and dashed lines are related to the PNR and click detectors, respectively. The overall losses correspond to efficiency $\eta=0.7$. The plots describe the cases: (a) N=5, r=0.57; (b) N=5, r=0.34; (c) N=3, r=0.57.

equalities. However, we do not prove here that they form the whole set of these inequalities.

We demonstrate the proposed method with phase-squeezed coherent states $|\alpha_0, r\rangle = \hat{D}(\alpha_0)\hat{S}(r)|0\rangle$. Here, $D(\alpha_0)$ is the displacement operator with $\alpha_0 \in \mathbb{R}$, $\hat{S}(r)$ is the squeeze operator with r > 0, and $|0\rangle$ is the vacuum state; cf. the inset in Fig. 2 for a contour line of the corresponding Wigner function. Such states exhibit super-Poissonian statistics of photocounts. Phase-insensitive measurements, like photocounting, and measurements of their amplitude quadrature are typically considered unsuitable for testing their nonclassicality [6].

The results in Fig. 2 challenge the prevailing intuition about the classical character of photocounting statistics for phase-squeezed coherent states. Contrary to this intuition, the statistics are found to be nonclassical, as evidenced by violations of tight Bell-like inequalities with N=3 and N=5 for both PNR and click detectors. While the Klyshko criterion can also demonstrate this nonclassicality, it is limited to PNR detectors. In contrast, our method can be employed with experimentally accessible click detectors.

IV. UNBALANCED HOMODYNE DETECTION

As mentioned, the binary measurement outcomes obtained with on-off detectors cannot be used for testing nonclassicality. However, the situation changes when the signal field is superposed with the local oscillator

field. The corresponding measurement procedure of unbalanced homodyne detection [47] is described by the behaviors of coherent states given by

$$\Pi(0|\alpha;\gamma_i) = \exp\left(-|\alpha - \gamma_i|^2\right),\tag{16}$$

where γ_i is the local-oscillator amplitude playing the role of the device setting. The dimensionality of the behaviors is equal to the number of settings. We chose it to be equal to two and denote $d = |\gamma_2 - \gamma_1|/2$. Similar to the examples above, all losses are assigned to quantum states. Another experimental imperfection, mode mismatch, according to its consideration in Ref. [68], leads to a multiplication of probabilities $\mathcal{P}(0|\gamma_i)$ and $\Pi(0|\alpha;\gamma_i)$ by a constant factor, depending on γ_i . It can be easily included in the consideration, cf. Appendix D 1, and even omitted, if $|\gamma_1| = |\gamma_2|$.

In the considered case, the space of coherent-state behaviors is given by a two-dimensional area, cf. Fig. 3, bounded by the curve parametrically defined as

$$\mathcal{P}(0|\gamma_1) = \Pi(0|t;\gamma_1) = \exp\left[-(t+d)^2\right],$$
 (17)

$$\mathcal{P}(0|\gamma_2) = \Pi(0|t;\gamma_2) = \exp\left[-(t-d)^2\right],$$
 (18)

where $t \in \mathbb{R}$. For $d \leq 1/\sqrt{2}$, this area represents the set of convex combinations of boundary points. Moreover, due to the non-zero gradient of $\Pi \cdot \lambda$ with respect to Π for $\lambda \neq 0$, we deduce

$$\sup_{\alpha \in \mathbb{C}} \mathbf{\Pi}(\alpha) \cdot \boldsymbol{\lambda} = \sup_{t \in \mathbb{R}} \mathbf{\Pi}(t) \cdot \boldsymbol{\lambda}, \tag{19}$$

where the components of $\Pi(t)$ are given by Eqs. (17) and (18). Details can be found in Appendixes D 2 and D 3. In particular, this implies that any classical statistic for unbalanced homodyne detection with two settings can be simulated with a single coherent state.

Summarizing the above considerations, we get that the tight Bell-like inequalities are obtained with

$$\lambda(t) = (\dot{\Pi}(0|t; \gamma_2) - \dot{\Pi}(0|t; \gamma_1)), \qquad (20)$$

i.e., are given by

$$-(t-d)e^{-(t-d)^2}\mathcal{P}(0|\gamma_1) + (t+d)e^{-(t+d)^2}\mathcal{P}(0|\gamma_2)$$

$$\leq 2de^{-2(t^2-d^2)}. (21)$$

These linear inequalities can be combined into three non-linear ones as

$$\sqrt{-\ln \mathcal{P}(0|\gamma_1)} + \sqrt{-\ln \mathcal{P}(0|\gamma_2)} \ge 2d, \qquad (22)$$

$$\sqrt{-\ln \mathcal{P}(0|\gamma_1)} + 2d \ge \sqrt{-\ln \mathcal{P}(0|\gamma_2)}, \tag{23}$$

$$\sqrt{-\ln \mathcal{P}(0|\gamma_2)} + 2d \ge \sqrt{-\ln \mathcal{P}(0|\gamma_1)}, \tag{24}$$

cf. Appendix D 3. Violation of at least one of them is a necessary and sufficient condition for nonclassicality of measurement statistics and a sufficient condition for nonclassicality of quantum states.

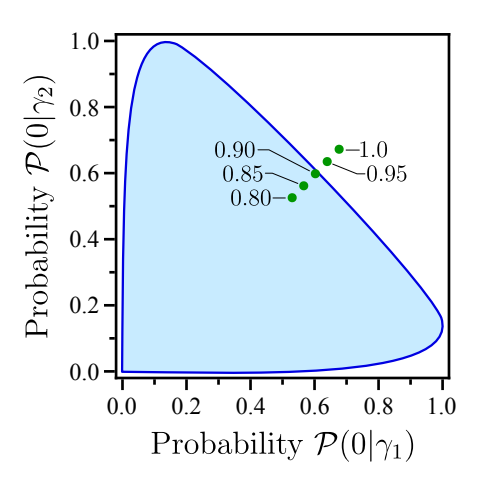


FIG. 3. The closed curve bounding the shaded two-dimensional area of the coherent-state behaviors in the case of unbalanced homodyne detection with two local-oscillator settings, $\gamma_{1,2}=\pm 1/\sqrt{2}$, is shown. Dots correspond to the behaviors for the squeezed vacuum states with r=0.34 and different efficiencies. The dots outside the classical area correspond to nonclassical behaviors.

We demonstrate the method with squeezed vacuum states $|r\rangle = \hat{S}(r) |0\rangle$. We have chosen the coherent displacements γ_1 and γ_2 in the direction of the anti-squeezed quadrature. The points in Fig. 3 outside the classical area correspond to nonclassical behaviors. In the considered scenario, this can also be interpreted as a nonclassicality of the photocounting statistics for two phase-squeezed coherent states, which is itself a counterintuitive fact. In this case it is tested with a single on-off detector.

V. SUMMARY AND CONCLUSIONS

We have considered nonclassicality of measurement statistics obtained in quantum-optical experiments. Nonclassicality, in this context, indicates that these statistics cannot be replicated using the same measurement device employed in the original experiment but with classical radiation fields at the source. It is important to note that this property, being important and interesting itself, is a sufficient condition for a broader concept—nonclassicality of quantum states.

We have used a mathematical similarity between two different phenomena—nonclassicality of measurement statistics in quantum optics and Bell nonlocality. Indeed, in both cases, we address a common question: whether the given behavior (the set of probability distributions of measurement outcomes for the used device settings) can be represented as a convex combination of other behaviors. They are deterministic behaviors in the context of Bell nonlocality. For nonclassicality of measurement statistics in quantum optics, the relevant behaviors are classical behaviors determined for coherent states of the radiation fields.

Bell inequalities are a powerful tool for testing Bell

nonlocality. Similarly, Bell-like inequalities have been introduced to test nonclassicality of measurement statistics. The problem is that the set of these inequalities, in the most general form, is not optimal and their application requires the use of involved optimization techniques. In this paper, we have shown that this problem can be significantly simplified by selecting the optimal set of these inequalities. Following the terminology used in the context of Bell nonlocality, we refer to them as tight inequalities.

First, we applied our method to photocounting statistics. In this context, we have considered two types of detectors: ideal PNR and realistic click detectors, i.e. arrays of on-off detectors. The simplest non-trivial scenario corresponds to two detectors in the array. In this case, we can combine all linear tight Bell-like inequalities into a single nonlinear one, which gives us a simple necessary and sufficient condition for nonclassicality of the photocounting statistics obtained with such a detection system.

An important scenario corresponds to the case with three and more detectors in the array. In particular, we have derived a subset of tight Bell-like inequalities for the case of an odd number of such detectors. The result is also applicable to a broad class of other detection techniques with an odd maximum number of clicks. In particular, we have considered the case of PNR detectors restricted by a given cut-off number of photons.

We have shown that our inequalities can demonstrate nonclassiacality of photocounting statistics for a counter-intuitive example—phase-squeezed coherent states. It is well known that such states are characterized by positive excess noise for photocounting statistics and amplitude quadrature. Photocounting measurements are typically considered inapplicable to test their nonclassicality. We have shown that this common intuition is generally incorrect. In fact, photocounting statistics of phase-squeezed coherent states are nonclassical. Moreover, our method enables it to be tested with minimal experimental resources

Next, we have considered a typical measurement, involving device settings—unbalanced homodyne detection. Restricting by use of an on-off detector and two settings of the local oscillators, we have derived a full set of tight Bell-like inequalities, which test nonclassicality of measurement statistics for this scenario. Moreover, we have shown that these linear inequalities are combined in three nonlinear ones.

The applicability of the method is shown for squeezed vacuum states. Again, we have considered a counterintuitive example—the local oscillator displaces this state in the direction of anti-squeezed quadrature. Intuitively, the corresponding behavior should not be nonclassical either. Indeed, these measurements can be interpreted as photocounting statistics for two phase-squeezed coherent states. However, we have shown that this intuition is also incorrect, and thus the behavior is nonclassical.

Therefore, we have proposed an efficient method for

testing nonclassicality of measurement statistics in quantum optics. We hope that this result will be useful for optical experiments testing quantum theory. We also believe that it could be useful for a deeper understanding of nonclassical resources in modern quantum technologies.

The authors acknowledge the National Research Foundation of Ukraine for supporting this work via the Project Nr. 2020.02/0111, Nonclassical and hybrid correlations of quantum systems under realistic conditions. A.A.S. thanks Boris Hage for enlightening discussions.

Appendix A: Derivation of Bell-like inequalities for nonclassicality of measurement statistics

In this section we remind the reader with the derivation of inequalities (2), introduced in Refs. [26, 58]. Applying Born's rule $\mathcal{P}(A|a) = \text{Tr}[\hat{\Pi}(A|a)\hat{\rho}]$ in Eq. (1) we get

$$\mathcal{P}(A|a) = \int_{\mathbb{C}} d^2 \alpha \, \Pi(A|a;\alpha) \, P(\alpha). \tag{A1}$$

Multiplying the above equation by an arbitrary $\lambda(A, a)$ and performing summation over A and a, we get

$$\sum_{a,A} \lambda(A,a) \mathcal{P}(A|a)$$

$$= \int_{\mathbb{C}} d^2 \alpha \left[\sum_{a,A} \lambda(a,A) \Pi(A|a;\alpha) \right] P(\alpha). \quad (A2)$$

If $P(\alpha) \geq 0$ and $\int_{\mathbb{C}} d^2 \alpha P(\alpha) = 1$, then $\forall f(\alpha)$

$$\int_{\mathbb{C}} d^2 \alpha f(\alpha) P(\alpha; s) \le \sup_{\alpha \in \mathbb{C}} f(\alpha)$$
 (A3)

according to the first mean-value theorem. Choosing $f(\alpha)=\sum\limits_{a,A}\lambda(A,a)\Pi\left(A|a;\alpha\right)$ and using Eq. (A2), we ob-

tain Bell-like inequalities (2). Furthermore, employing the Farkas lemma [69], one can prove that if these inequalities are satisfied, then there exist such $P(\alpha) \geq 0$ that Eq. (A1) is satisfied. Importantly, this function may not be the same as the P-function. Consequently, non-classicality of measurement statistics always implies non-classicality of quantum states, but the reverse is generally not true.

Appendix B: General statements on tight Bell-like inequalities

1. Closed convex cones

We start with a proof of the fact that $L(\alpha)$ defined by Eq. (5) forms a closed convex cone. If λ_1 and $\lambda_2 \in$ $L(\alpha)$, then their conic combination $C_1\lambda_1 + C_2\lambda_2$, where $C_1, C_2 \geq 0$, also belongs to $L(\alpha)$, since the sum of two functions that share a global maximum point reaches its global maximum at that point. This proves that $L(\alpha)$ is a convex cone. In order to prove that it is closed, consider an arbitrary convergent sequence $\lambda_n \in L(\alpha)$, $n \in \mathbb{N}$. Since for any n and $\alpha' \in \mathbb{C}$

$$\Pi(\alpha) \cdot \lambda_n \ge \Pi(\alpha') \cdot \lambda_n,$$
 (B1)

the same property holds for the limit of the sequence

$$\Pi(\alpha) \cdot \tilde{\lambda} \ge \Pi(\alpha') \cdot \tilde{\lambda}, \quad \tilde{\lambda} = \lim_{n \to +\infty} \lambda_n.$$
 (B2)

Thus, any convergent sequence in $L(\alpha)$ has its limit also in $L(\alpha)$, which proves that $L(\alpha)$ is closed.

2. Proof of Statement 1

Next, we prove Statement 1. For this purpose, we first suppose that the set Λ is defined by Eq. (6). We have to show that the two conditions from Definition 1 are satisfied for this set.

Let us start with Condition (i). Suppose that $\lambda' \notin \Lambda$ and $\arg\max_{\alpha \in \mathbb{C}_{\infty}} \Pi(\alpha) \cdot \lambda' = \alpha'$. We have to prove that the corresponding Bell-like inequality follows from the inequalities given by the test functions from Λ . The definition of extreme rays yields

$$\lambda' = \sum_{\lambda_i \in L(\alpha')} C_i \lambda_i, \tag{B3}$$

where $C_i \geq 0$. This implies that

$$\mathcal{P} \cdot \lambda' = \sum_{\lambda_i \in L(\alpha')} C_i \mathcal{P} \cdot \lambda_i$$

$$\leq \sum_{\lambda_i \in L(\alpha')} C_i \sup_{\alpha \in \mathbb{C}} \Pi(\alpha) \cdot \lambda_i$$

$$= \sum_{\lambda_i \in L(\alpha')} C_i \Pi(\alpha') \cdot \lambda_i = \Pi(\alpha') \cdot \lambda'$$

$$= \sup_{\alpha \in \mathbb{C}} \Pi(\alpha) \cdot \lambda'. \tag{B4}$$

Thus, the Bell-like inequality associated with λ' follows from the ones corresponding to test functions from $L(\alpha')$.

Next, we prove Condition (ii). Suppose that there is $\lambda' \in \operatorname{Ext}[L(\alpha')] \subset \Lambda$ such that the corresponding Bell-like inequality follows from inequalities associated with some test functions from Λ . Then

$$\lambda' = \sum_{i=1}^{n} C_i \lambda_i, \quad C_i > 0, \quad \lambda_i \in \Lambda,$$
 (B5)

and

$$\mathcal{P} \cdot \lambda' = \sum_{i=1}^{n} C_i \mathcal{P} \cdot \lambda_i \le \sum_{i=1}^{n} C_i \sup_{\alpha \in \mathbb{C}} \Pi(\alpha) \cdot \lambda_i.$$
 (B6)

At the same time, the right-hand-side of this inequality fulfills the condition

$$\sum_{i=1}^{n} C_{i} \sup_{\alpha \in \mathbb{C}} \mathbf{\Pi}(\alpha) \cdot \boldsymbol{\lambda}_{i} \ge \sup_{\alpha \in \mathbb{C}} \sum_{i} C_{i} \mathbf{\Pi}(\alpha) \cdot \boldsymbol{\lambda}_{i}$$
$$= \sup_{\alpha \in \mathbb{C}} \mathbf{\Pi}(\alpha) \cdot \boldsymbol{\lambda}'. \tag{B7}$$

Therefore, the inequality for λ' can be inferred from the inequalities for λ_i only if the equality

$$\sum_{i=1}^{n} C_{i} \sup_{\alpha \in \mathbb{C}} \mathbf{\Pi}(\alpha) \cdot \boldsymbol{\lambda}_{i} = \sup_{\alpha \in \mathbb{C}} \sum_{i=1}^{n} C_{i} \mathbf{\Pi}(\alpha) \cdot \boldsymbol{\lambda}_{i}$$
 (B8)

is satisfied. This implies

$$\sup_{\alpha \in \mathbb{C}} \mathbf{\Pi}(\alpha) \cdot \boldsymbol{\lambda}_i = \mathbf{\Pi}(\alpha') \cdot \boldsymbol{\lambda}_i$$
 (B9)

for all $i = 1 \dots n$.

Indeed, let us assume that Eq. (B8) is satisfied and, without loss of generality, Eq. (B9) is not satisfied for λ_j , $j = 1 \dots k \leq n$. Hence, these λ_j fulfill the condition

$$\sup_{\alpha \in \mathbb{C}} \mathbf{\Pi}(\alpha) \cdot \boldsymbol{\lambda}_j = \mathbf{\Pi}(\alpha_j) \cdot \boldsymbol{\lambda}_j > \mathbf{\Pi}(\alpha') \cdot \boldsymbol{\lambda}_j.$$
 (B10)

This yields

$$\sum_{i=1}^{n} \sup_{\alpha \in \mathbb{C}} C_{i} \mathbf{\Pi}(\alpha) \cdot \boldsymbol{\lambda}_{i}$$

$$= \sum_{j=1}^{k} C_{j} \mathbf{\Pi}(\alpha_{j}) \cdot \boldsymbol{\lambda}_{j} + \sum_{i=k+1}^{n} C_{i} \mathbf{\Pi}(\alpha') \cdot \boldsymbol{\lambda}_{i}.$$
(B11)

On the other hand, Eq. (B8) implies

$$\sum_{i=1}^{n} \sup_{\alpha \in \mathbb{C}} C_i \mathbf{\Pi}(\alpha) \cdot \boldsymbol{\lambda}_i = \sum_{i=1}^{n} C_i \mathbf{\Pi}(\alpha') \cdot \boldsymbol{\lambda}_i.$$
 (B12)

Equating these expressions we obtain the equality

$$\sum_{j=1}^{k} C_j \mathbf{\Pi}(\alpha_j) \cdot \boldsymbol{\lambda}_j = \sum_{j=1}^{k} C_j \mathbf{\Pi}(\alpha') \cdot \boldsymbol{\lambda}_j.$$
 (B13)

However, it contradicts the assumption $\Pi(\alpha_j) \cdot \lambda_j > \Pi(\alpha') \cdot \lambda_j$. This implies

$$\sup_{\alpha \in \mathbb{C}} \mathbf{\Pi}(\alpha) \cdot \boldsymbol{\lambda}_i = \mathbf{\Pi}(\alpha') \cdot \boldsymbol{\lambda}_i, \tag{B14}$$

where $i = 1 \dots n$, that is $\lambda_i \in L(\alpha')$.

This means that λ' is a conic combination of other test functions from Ext $[L(\alpha')]$. This conclusion violates the assumption that λ' belongs to Ext $[L(\alpha')]$. Thus, the inequality for λ' cannot be inferred from other tight Bell-like inequalities.

Appendix C: Tight inequalities for photocounting with odd N

1. Hodge star

Let us first elaborate on the usage of the Hodge star \star and the wedge symbol \wedge . For our purposes, we only need to evaluate the expression $\boldsymbol{u} = \star \bigwedge_{i=1}^{n-1} \boldsymbol{v}^i$, where $\boldsymbol{v}^i \in \mathbb{R}^n$. In such a case \boldsymbol{u} is also a vector from \mathbb{R}^n given by

$$\star \bigwedge_{i=1}^{n-1} \mathbf{v}^{i} = \begin{vmatrix} \mathbf{e}^{1} & \mathbf{e}^{2} & \dots & \mathbf{e}^{n} \\ v_{1}^{1} & v_{2}^{1} & \dots & v_{n}^{1} \\ \vdots & \vdots & \ddots & \vdots \\ v_{1}^{n-1} & v_{2}^{n-1} & \dots & v_{n}^{n-1} \end{vmatrix}, \tag{C1}$$

where $\{e^1, e^2, \dots, e^n\}$ is the standard basis in \mathbb{R}^n , i.e., $e^i_j = \delta_{ij}$. In other words, \boldsymbol{u} is a generalized cross product of n-1 vectors in an n-dimensional space.

2. Proof of Statement 2

Without loss of generality, let us assume that $\tau = 0$. Equation (14) together with Rolle's theorem implies that $\dot{\mathbf{\Pi}}(t) \cdot \boldsymbol{\lambda}(t;\tau)$ equals zero at the points $c_1 \in]0, t_1[, c_2 \in]t_1, t_2[, \ldots, c_m \in]t_{m-1}, t_m[; \text{ cf. Fig. 1. Together with }t_1, \ldots, t_m, \text{ these points exhaust the }2m \text{ zeros of }\dot{\mathbf{\Pi}}(t) \cdot \boldsymbol{\lambda}(t;\tau) \text{ as a function of }t.$

Since the derivatives $\dot{\mathbf{\Pi}}(t) \cdot \boldsymbol{\lambda}(\boldsymbol{t};\tau)$ are equal for all $t=t_i$ and $t=c_i$, the 2m-1 zeros of $\ddot{\mathbf{\Pi}}(t) \cdot \boldsymbol{\lambda}(\boldsymbol{t};\tau)$ are located at $]c_1,t_1[,\ldots,]c_m,t_m[$ according to Rolle's theorem. Therefore, we get $\ddot{\mathbf{\Pi}}(t_i) \cdot \boldsymbol{\lambda}(\boldsymbol{t};\tau) \neq 0$ for $i=1\ldots m$. This implies that the points $t_1,\ldots,t_m,c_1,\ldots,c_m$ are extrema of $\mathbf{\Pi}(t) \cdot \boldsymbol{\lambda}(\boldsymbol{t};\tau)$.

Let us set such a sign of $\lambda(t;\tau)$ that $t=\tau=0$ is a local maximum of $\Pi(t)\cdot\lambda(t;\tau)$ at [0,1]. The nearest extremum is c_1 , which consequently must be a local minimum. It yields that t_1 is a local maximum. This pattern is repeated up until t_m , which proves that τ, t_1, \ldots, t_m are maxima points. By conditions of this Statement there are no other critical points at]0,1[. Consequently, there are no other points, which could be the global maximum. Finally, one has to consider the other endpoint $t=1-\tau=1$. Since t_m is a local maximum and there are no extrema in $]t_m, 1-\tau[$, the point $t=1-\tau$ is a local minimum.

3. Conditions of Statement 2 for PNR and click detectors

Let us prove that this condition is satisfied by the photon-number resolving (PNR) and click detectors. We start with the PNR detectors. For convenience, we use here another parametrization, $s = e^{-|\alpha|^2}$, related to our standard parametrization, $t = e^{-|\alpha|^2/N}$, via the monotonic function $s = t^N$. In this case, the components of

the coherent-state behaviors are given by

$$\Pi(n|s) = s \frac{(-\ln s)^n}{n!}.$$
 (C2)

This yields,

$$\Pi(s) \cdot \lambda(s; \tau) = sP(-\ln s), \tag{C3}$$

where $P(-\ln s)$ is a 2m-th degree polynomial in terms of $-\ln s$. The first derivative,

$$\dot{\mathbf{\Pi}}(s) \cdot \boldsymbol{\lambda}(s;\tau) = P(-\ln s) - P'(-\ln s), \tag{C4}$$

has 2m zeros. Therefore, apart from $s_1, \ldots s_m$, the function $\Pi(s) \cdot \lambda(s, \tau)$ has m other critical points at $s \in]0, 1[$. The second derivative reads

$$\ddot{\mathbf{\Pi}}(s) \cdot \boldsymbol{\lambda}(s;\tau) = \frac{P''(-\ln s) - P'(-\ln s)}{s}.$$
 (C5)

It has no more than 2m-1 zeros, since the nominator in this equation is a (2m-1)-th degree polynomial. Since the parameters s and t are related through a monotonic function, these conclusions also holds for the latter.

Next, we consider the click detectors with the components of the coherent-state behaviors given by

$$\Pi(n|t) = \binom{N}{n} t^{N-n} (1-t)^n.$$
 (C6)

Then $\Pi(t) \cdot \lambda(t;\tau)$ is a (2m+1)-th degree polynomial, which has no more than 2m critical points and whose second derivative has no more than 2m-1 zeros.

4. Extreme-ray condition

In Sec. IIIB we have applied a statement from the convex analysis, which can be formulated based on results presented in Ref. [61]. For convenience, we also present it here in notations of this paper.

Statement 3. Suppose a vector $\lambda \in L$. Then it belongs to Ext [L] iff it is not a conic combination of any other two vectors λ_1 , $\lambda_2 \in L$, i.e. $\lambda \neq C_1\lambda_1 + C_2\lambda_2$, $C_1, C_2 > 0$, where $\lambda_i \neq b_i\lambda$, $b_i > 0$, i = 1, 2.

Proof. Suppose that there exists $\lambda \in \text{Ext } L$ such that

$$\lambda = C_1 \lambda_1 + C_2 \lambda_2, \quad c_1, c_2 > 0, \tag{C7}$$

for some λ_1 , λ_2 , where $\lambda_i \neq b_i \lambda$, $b_i > 0$, i = 1, 2. Utilizing

$$\lambda_i = \sum_{\lambda' \in \text{Ext}[L]} a_i(\lambda') \lambda', \tag{C8}$$

where $a_i(\lambda') \geq 0$, i = 1, 2, one can obtain

$$\lambda = \sum_{\lambda' \in \text{Ext}[L]} \left(C_1 a_1(\lambda') + C_2 a_2(\lambda') \right) \lambda'.$$
 (C9)

Since $\lambda \in \operatorname{Ext}[L]$, $C_1a_1(\lambda') + C_2a_2(\lambda') = 0$ for $\lambda' \neq \lambda$. Then $a_1(\lambda') = a_2(\lambda') = 0$ if $\lambda' \neq \lambda$. But this yields $\lambda_i = a_i(\lambda)\lambda$, which contradicts the initial assumption.

In order to prove the converse statement, recall that any test function from L can be expressed as a conic combination of the test functions from $\operatorname{Ext}[L]$. But the only possible conic combination representation of λ is λ itself. Therefore, $\lambda \in \operatorname{Ext}[L]$.

Appendix D: Tight inequalities for unbalanced homodyne detection

1. Mode mismatch

In order to consider the effect of mode mismatch, we remind the corresponding coherent-state behavior, cf. Ref. [68] in the main text,

$$\Pi(0|\alpha;\gamma;\eta;\xi) = e^{-\eta|\alpha-\gamma|^2} e^{-|\gamma|^2 \eta^{\frac{1-\xi}{\xi}}}, \quad (D1)$$

where the mode mismatch parameter $\xi \in [0,1]$ and the detection efficiency $\eta \in [0,1]$. By defining a new parameter $\beta = \sqrt{\eta}\alpha$ it can be rewritten as

$$\Pi(0|\beta;\gamma;\eta;\xi) = e^{-|\beta - \sqrt{\eta}\gamma|^2} e^{-|\sqrt{\eta}\gamma|^2 \frac{1-\xi}{\xi}}.$$
 (D2)

This is effectively the coherent-state behavior for the coherent displacement $\sqrt{\eta}\gamma$ multiplied by the factor

$$g(\gamma; \eta; \xi) = e^{-|\sqrt{\eta}\gamma|^2 \frac{1-\xi}{\xi}}$$
 (D3)

Let us find the tight Bell-like inequalities for the scenario with coherent displacements γ_1 , γ_2 , the efficiency η , and the mode mismatch parameter ξ . Since the coherent displacements are effectively $\sqrt{\eta}\gamma_1$ and $\sqrt{\eta}\gamma_2$, we can make use of the tight test functions for the case with these settings. In order to account for the factor

$$e^{-|\sqrt{\eta}\gamma|^2 \frac{1-\xi}{\xi}},$$
 (D4)

we can multiply the corresponding elements of the test functions by the inverse factors. More specifically, a test function $\lambda = \{\lambda_1, \lambda_2\}$ becomes

$$\lambda' = \left\{ \frac{1}{g(\gamma_1; \eta; \xi)} \lambda_1, \frac{1}{g(\gamma_2; \eta; \xi)} \lambda_2 \right\}.$$
 (D5)

Therefore, the right-hand side of such Bell-like inequalities reads

$$\Pi(0|\beta;\gamma_1;\eta;\xi)\lambda_1' + \Pi(0|\beta;\gamma_2;\eta;\xi)\lambda_2' =$$

$$=\Pi(0|\beta;\sqrt{\eta}\gamma_1;1;1)\lambda_1 + \Pi(0|\beta;\sqrt{\eta}\gamma_2;1;1)\lambda_2, \quad (D6)$$

which have been proved to be tight.

2. Boundary supremum

Consider the right-hand side of a Bell-like inequality, $\sup_{\alpha \in \mathbb{C}} \Pi(\alpha) \cdot \lambda$, in the case of unbalanced homodyne detection with two settings. In order to calculate the supremum, let us make a change of variables $\boldsymbol{w} = \Pi(\alpha)$ so that

$$\sup_{\alpha \in \mathbb{C}} \mathbf{\Pi}(\alpha) \cdot \boldsymbol{\lambda} = \sup_{\boldsymbol{w} \in W} \boldsymbol{w} \cdot \boldsymbol{\lambda} = \sup_{\boldsymbol{w} \in W} \boldsymbol{w} \cdot \boldsymbol{\lambda}, \quad (D7)$$

where $W = \{\mathbf{\Pi}(\alpha) | \alpha \in \mathbb{C}_{\infty}\}$. Then $\nabla_{w_i} (\boldsymbol{w} \cdot \boldsymbol{\lambda}) = \lambda_i$ for i = 1, 2. These partial derivatives equal zero simultaneously iff $\lambda_i = 0$, i = 1, 2, which is a trivial case. Otherwise,

$$\sup_{\boldsymbol{w} \in W} \boldsymbol{w} \cdot \boldsymbol{\lambda} = \sup_{\boldsymbol{w} \in \partial W} \boldsymbol{w} \cdot \boldsymbol{\lambda}, \tag{D8}$$

i.e. the maximum value of $\boldsymbol{w} \cdot \boldsymbol{\lambda}$ is reached at the boundary ∂W of W.

3. Derivation of tight inequalities

Let us calculate the boundary ∂W . Suppose that $\mathcal{P} \in W$, where $\mathcal{P} = (\mathcal{P}(0|\gamma_1) \ \mathcal{P}(0|\gamma_2))$. Then

$$\mathcal{P}(0|\gamma_i) = \exp\left(-\left|\alpha - \gamma_i\right|^2\right),\tag{D9}$$

which implies

$$|\alpha - \gamma_i|^2 = -\ln \mathcal{P}(0|\gamma_i), \quad i = 1, 2.$$
 (D10)

The two equations correspond to the circles in the α plane with radii $\sqrt{-\ln \mathcal{P}(0|\gamma_1)}$ and $\sqrt{-\ln \mathcal{P}(0|\gamma_2)}$, cf. Fig. 4. If this system of equations has a solution α , the two circles have at least one intersection point. Such an intersection point and the two centers form a triangle with the sides that equal $\sqrt{-\ln \mathcal{P}(0|\gamma_1)}$, $\sqrt{-\ln \mathcal{P}(0|\gamma_2)}$ and $2d = |\gamma_1 - \gamma_2|$, which yields the triangle inequalities (22-24).

The inequalities are non-strict, since if the triangle degenerates into a line, the two circles still have an intersection point. In this case, the probability values belong to the boundary ∂W . The latter can be parameterized by Eqs. (17) and (18). Indeed, by substituting this parametrization in the triangle inequalities, we find that inequalities (23), (22), and (24) become equalities for $t \leq -d$, $|t| \leq d$, and $t \geq d$, respectively. Two other inequalities are trivially satisfied in these cases. This yields Eq. (19) and $L(t) \equiv L(\Pi(t))$. Here the components of $\Pi(t)$ are given by Eqs. (17) and (18).

Next, we consider properties of the curve, corresponding to the boundary ∂W . Let $\theta(t)$ be the tangential angle of the curve at the point $\Pi(t)$, i.e., the polar angle of

$$\dot{\mathbf{\Pi}}(t) = -2\left([t+d]\Pi(0|t;\gamma_1) \ [t-d]\Pi(0|t;\gamma_2)\right).$$
 (D11)

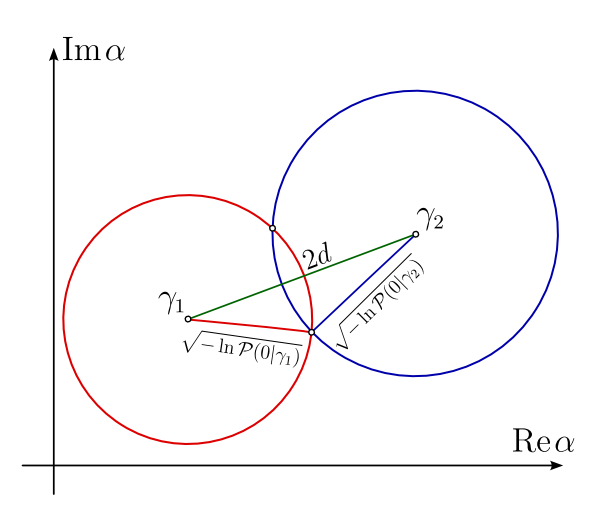


FIG. 4. The circles, corresponding to Eq. (D10), and the triangle, demonstrating inequalities (22-24) are shown.

Firstly, note that

$$\frac{\dot{\mathbf{\Pi}}(-\infty)}{\left|\dot{\mathbf{\Pi}}(-\infty)\right|} = \begin{pmatrix} 1 & 0 \end{pmatrix} \quad \text{and} \quad \frac{\dot{\mathbf{\Pi}}(+\infty)}{\left|\dot{\mathbf{\Pi}}(+\infty)\right|} = \begin{pmatrix} 0 & -1 \end{pmatrix}.$$
(D12)

This implies $\theta(-\infty) = 0$ and $\theta(+\infty) = 3\pi/2$. Secondly, since $\Pi(0|t;\gamma_1), \Pi(0|t;\gamma_2) \geq 0$, it is evident that the conditions $\dot{\Pi}(0|t;\gamma_1) > 0$, $\dot{\Pi}(0|t;\gamma_2) < 0$ can never hold simultaneously. This implies that $0 \leq \theta(t) \leq 3\pi/2$. Thirdly, the tangential angle can be represented as

$$\theta(t) = \tag{D13}$$

$$\int_{-\infty}^{t} \frac{\dot{\Pi}(0|t';\gamma_{1})\ddot{\Pi}(0|t';\gamma_{2}) - \dot{\Pi}(0|t';\gamma_{2})\ddot{\Pi}(0|t';\gamma_{1})}{\left|\dot{\Pi}(t')\right|^{2}} dt'.$$

Consider the quantity

$$\begin{split} &\dot{\Pi}(0|t;\gamma_1)\ddot{\Pi}(0|t;\gamma_2) - \dot{\Pi}(0|t;\gamma_2)\ddot{\Pi}(0|t;\gamma_1) \\ &= 16\Pi(0|t;\gamma_1)\Pi(0|t;\gamma_2)d\left(t^2 - d^2 + \frac{1}{2}\right). \end{split} \label{eq:definition}$$

If $d \leq 1/\sqrt{2}$, this expression is non-negative, and hence $\dot{\theta}(t) \geq 0$. In other words, $\theta(t)$ is a monotonic function in this case.

Let us calculate L(t) for $t \in \mathbb{R}$. We focus on the case when $d \leq 1/\sqrt{2}$. If

$$\underset{t' \in \mathbb{R}_{\infty}}{\operatorname{arg\,max}} \, \mathbf{\Pi}(t') \cdot \boldsymbol{\lambda} = t, \tag{D15}$$

then

$$\frac{\partial}{\partial t'} \left[\mathbf{\Pi}(t') \cdot \boldsymbol{\lambda}(t) \right]_{t'=t} = \dot{\mathbf{\Pi}}(t) \cdot \boldsymbol{\lambda}(t) = 0. \tag{D16}$$

This yields

$$\lambda(t) = C\left(\dot{\Pi}(0|t;\gamma_2) - \dot{\Pi}(0|t;\gamma_1)\right),\tag{D17}$$

 $C \in \mathbb{R}$. Consider the second derivative

$$\begin{split} &\frac{\partial^2}{\partial t'^2} \big[\boldsymbol{\Pi}(t') \cdot \boldsymbol{\lambda}(t) \big]_{t'=t} = \ddot{\boldsymbol{\Pi}}(t) \cdot \boldsymbol{\lambda}(t) \\ &= C \left[\dot{\boldsymbol{\Pi}}(0|t; \gamma_2) \ddot{\boldsymbol{\Pi}}(0|t; \gamma_1) - \dot{\boldsymbol{\Pi}}(0|t; \gamma_1) \ddot{\boldsymbol{\Pi}}(0|t; \gamma_2) \right] \\ &\propto C \dot{\boldsymbol{\theta}}(t). \end{split} \tag{D18}$$

The expression inside the brackets is positive for $d < 1/\sqrt{2}$, cf. Eq. (D14). Hence, the sign of the second derivative is determined by the sign of C. For t to be a local maximum of $\Pi(t') \cdot \lambda(t)$ as a function of t', it is sufficient that the second derivative is negative, and hence C > 0.

If $d=1/\sqrt{2}$, the second derivative is zero, therefore we should consider this case separately. For $t \neq 0$, Eq. (D18) is still negative for C > 0. If t = 0, one directly can check that

$$\frac{\partial^3}{\partial t'^3} \left[\mathbf{\Pi}(t') \cdot \boldsymbol{\lambda}(0) \right]_{t'=0} = 0 \tag{D19}$$

and

$$\frac{\partial^4}{\partial t'^4} \left[\mathbf{\Pi}(t') \cdot \boldsymbol{\lambda}(0) \right]_{t'=0} = -C \frac{16\sqrt{2}}{e}, \tag{D20}$$

which is negative if C > 0. This ensures that t' = 0 is a local maximum of $\Pi(t') \cdot \lambda(0)$.

Suppose that there is another extremum of $\Pi(t') \cdot \lambda(t)$ as a function of t' at the point $t' = s \neq t$. The condition

$$\frac{\partial}{\partial t'} \left[\mathbf{\Pi}(t') \cdot \boldsymbol{\lambda}(t) \right]_{t'=s} = \dot{\mathbf{\Pi}}(s) \cdot \boldsymbol{\lambda}(t) = 0$$
 (D21)

requires that $\dot{\mathbf{\Pi}}(s) = B\dot{\mathbf{\Pi}}(t)$, $B \neq 0$ since both $\dot{\mathbf{\Pi}}(s)$ and $\dot{\mathbf{\Pi}}(t)$ are orthogonal to $\boldsymbol{\lambda}(t)$. The condition $s \neq t$ implies that B < 0. Indeed, B > 0 yields $\theta(s) = \theta(t)$ since the vectors $\dot{\mathbf{\Pi}}(t)$ and $\dot{\mathbf{\Pi}}(s)$ are co-directed. Hence, s = t, since $\theta(t')$ is a monotonic function. The second derivative at this point is positive, i.e.,

$$\frac{\partial^2}{\partial t'^2} \left[\mathbf{\Pi}(t') \cdot \boldsymbol{\lambda}(t) \right]_{t'=s} = \ddot{\mathbf{\Pi}}(s) \cdot \boldsymbol{\lambda}(t)$$
$$= B \ddot{\mathbf{\Pi}}(t) \cdot \boldsymbol{\lambda}(t) > 0, \tag{D22}$$

indicating that t' = s is the point of a local minimum.

Finally, in order to prove that t' = t corresponds to the global maximum of $\Pi(t') \cdot \lambda(t)$, we need to consider the infinite point $t = \infty$. We employ the property

$$\mathbf{\Pi}(\infty) \cdot \boldsymbol{\lambda}(t) = 0 < \mathbf{\Pi}(t) \cdot \boldsymbol{\lambda}(t) = 4Ce^{2t^2 + 2d^2}d. \quad (D23)$$

This implies that

$$L(t) = \{ C \left(\dot{\Pi}_2(t) - \dot{\Pi}_1(t) \right) | C > 0 \}.$$
 (D24)

Therefore, the extreme rays of L(t) are given by

$$\operatorname{Ext} L(t) = \left\{ \left(\dot{\Pi}_2(t) - \dot{\Pi}_1(t) \right) \right\}, \tag{D25}$$

which defines tight Bell-like inequalities.

- [1] U. M. Titulaer and R. J. Glauber, Correlation functions for coherent fields, Phys. Rev. **140**, B676 (1965).
- [2] L. Mandel, Non-classical states of the electromagnetic field, Phys. Scr. T12, 34 (1986).
- [3] L. Mandel and E. Wolf, Optical Coherence and Quantum Optics (Cambridge University Press, Cambridge, 1995).
- [4] W. Vogel and D.-G. Welsch, Quantum Optics (Wiley-VCH Verlag GmbH & Co. KGaA, 2006).
- [5] G. S. Agarwal, Quantum Optics (Cambridge University Press, Cambridge, 2013).
- [6] R. Schnabel, Squeezed states of light and their applications in laser interferometers, Phys. Rep. 684, 1 (2017).
- [7] J. Sperling and I. A. Walmsley, Quasiprobability representation of quantum coherence, Phys. Rev. A 97, 062327 (2018).
- [8] J. Sperling and I. A. Walmsley, Quasistates and quasiprobabilities, Phys. Rev. A 98, 042122 (2018).
- [9] J. Sperling and W. Vogel, Quasiprobability distributions for quantum-optical coherence and beyond, Phys. Scr. 95, 034007 (2020).
- [10] R. J. Glauber, Coherent and incoherent states of the radiation field, Phys. Rev. 131, 2766 (1963).
- [11] E. C. G. Sudarshan, Equivalence of semiclassical and quantum mechanical descriptions of statistical light beams, Phys. Rev. Lett. 10, 277 (1963).
- [12] T. Kiesel, W. Vogel, V. Parigi, A. Zavatta, and M. Bellini, Experimental determination of a nonclassical Glauber-Sudarshan P function, Phys. Rev. A 78, 021804(R) (2008).
- [13] T. Kiesel, W. Vogel, M. Bellini, and A. Zavatta, Nonclassicality quasiprobability of single-photon-added thermal states, Phys. Rev. A 83, 032116 (2011).
- [14] T. Kiesel and W. Vogel, Nonclassicality filters and quasiprobabilities, Phys. Rev. A 82, 032107 (2010).
- [15] E. Agudelo, J. Sperling, and W. Vogel, Quasiprobabilities for multipartite quantum correlations of light, Phys. Rev. A 87, 033811 (2013).
- [16] A. Luis, J. Sperling, and W. Vogel, Nonclassicality phasespace functions: More insight with fewer detectors, Phys. Rev. Lett. 114, 103602 (2015).
- [17] M. Bohmann and E. Agudelo, Phase-space inequalities beyond negativities, Phys. Rev. Lett. 124, 133601 (2020).
- [18] M. Bohmann, E. Agudelo, and J. Sperling, Probing nonclassicality with matrices of phase-space distributions, Quantum 4, 343 (2020).
- [19] M. Hillery, Nonclassical distance in quantum optics, Phys. Rev. A 35, 725 (1987).
- [20] C. T. Lee, Measure of the nonclassicality of nonclassical states, Phys. Rev. A 44, R2775 (1991).
- [21] J. K. Asbóth, J. Calsamiglia, and H. Ritsch, Computable measure of nonclassicality for light, Phys. Rev. Lett. 94, 173602 (2005).
- [22] A. Miranowicz, K. Bartkiewicz, A. Pathak, J. Peřina, Y.-N. Chen, and F. Nori, Statistical mixtures of states can be more quantum than their superpositions: Comparison of nonclassicality measures for single-qubit states, Phys. Rev. A 91, 042309 (2015).
- [23] A. Miranowicz, K. Bartkiewicz, N. Lambert, Y.-N. Chen, and F. Nori, Increasing relative nonclassicality quantified by standard entanglement potentials by dissipation and unbalanced beam splitting, Phys. Rev. A 92, 062314

- (2015).
- [24] B. Yadin, F. C. Binder, J. Thompson, V. Narasimhachar, M. Gu, and M. S. Kim, Operational resource theory of continuous-variable nonclassicality, Phys. Rev. X 8, 041038 (2018).
- [25] S. Luo and Y. Zhang, Quantifying nonclassicality via Wigner-Yanase skew information, Phys. Rev. A 100, 032116 (2019).
- [26] A. A. Semenov and A. B. Klimov, Dual form of the phasespace classical simulation problem in quantum optics, New J. Phys. 23, 123046 (2021).
- [27] M. D. Reid and D. F. Walls, Violations of classical inequalities in quantum optics, Phys. Rev. A 34, 1260 (1986).
- [28] A. Rivas and A. Luis, Nonclassicality of states and measurements by breaking classical bounds on statistics, Phys. Rev. A 79, 042105 (2009).
- [29] J. Peřina, V. Michálek, and O. Haderka, Non-classicality of optical fields as observed in photocount and photonnumber distributions, Opt. Express 28, 32620 (2020).
- [30] L. Innocenti, L. Lachman, and R. Filip, Coherence-based operational nonclassicality criteria, Phys. Rev. Lett. 131, 160201 (2023).
- [31] L. Mandel, Sub-Poissonian photon statistics in resonance fluorescence, Opt. Lett. 4, 205 (1979).
- [32] G. S. Agarwal and K. Tara, Nonclassical character of states exhibiting no squeezing or sub-Poissonian statistics, Phys. Rev. A 46, 485 (1992).
- [33] D. N. Klyshko, Observable signs of nonclassical light, Phys. Lett. A 213, 7 (1996).
- [34] J. Sperling, W. Vogel, and G. S. Agarwal, Sub-binomial light, Phys. Rev. Lett. 109, 093601 (2012).
- [35] T. J. Bartley, G. Donati, X.-M. Jin, A. Datta, M. Barbieri, and I. A. Walmsley, Direct observation of sub-binomial light, Phys. Rev. Lett. 110, 173602 (2013).
- [36] J. Sperling, W. Vogel, and G. S. Agarwal, Correlation measurements with on-off detectors, Phys. Rev. A 88, 043821 (2013).
- [37] H. Paul, P. Törmä, T. Kiss, and I. Jex, Photon chopping: New way to measure the quantum state of light, Phys. Rev. Lett. 76, 2464 (1996).
- [38] S. A. Castelletto, I. P. Degiovanni, V. Schettini, and A. L. Migdall, Reduced deadtime and higher rate photoncounting detection using a multiplexed detector array, J. Mod. Opt. 54, 337 (2007).
- [39] V. Schettini, S. V. Polyakov, I. P. Degiovanni, G. Brida, S. Castelletto, and A. L. Migdall, Implementing a multiplexed system of detectors for higher photon counting rates, IEEE J. Sel. Top. Quantum Electron. 13, 978 (2007).
- [40] J.-L. Blanchet, F. Devaux, L. Furfaro, and E. Lantz, Measurement of sub-shot-noise correlations of spatial fluctuations in the photon-counting regime, Phys. Rev. Lett. 101, 233604 (2008).
- [41] D. Achilles, C. Silberhorn, C. Śliwa, K. Banaszek, and I. A. Walmsley, Fiber-assisted detection with photon number resolution, Opt. Lett. 28, 2387 (2003).
- [42] M. J. Fitch, B. C. Jacobs, T. B. Pittman, and J. D. Franson, Photon-number resolution using time-multiplexed single-photon detectors, Phys. Rev. A 68, 043814 (2003).
- [43] J. Řeháček, Z. Hradil, O. Haderka, J. Peřina, and

- M. Hamar, Multiple-photon resolving fiber-loop detector, Phys. Rev. A $\bf 67$, 061801(R) (2003).
- [44] J. Sperling, W. Vogel, and G. S. Agarwal, True photocounting statistics of multiple on-off detectors, Phys. Rev. A 85, 023820 (2012).
- [45] J. Park, J. Zhang, J. Lee, S.-W. Ji, M. Um, D. Lv, K. Kim, and H. Nha, Testing nonclassicality and non-Gaussianity in phase space, Phys. Rev. Lett. 114, 190402 (2015).
- [46] J. Park and H. Nha, Demonstrating nonclassicality and non-Gaussianity of single-mode fields: Bell-type tests using generalized phase-space distributions, Phys. Rev. A 92, 062134 (2015).
- [47] S. Wallentowitz and W. Vogel, Unbalanced homodyning for quantum state measurements, Phys. Rev. A 53, 4528 (1996).
- [48] L.-A. Wu, H. J. Kimble, J. L. Hall, and H. Wu, Generation of squeezed states by parametric down conversion, Phys. Rev. Lett. 57, 2520 (1986).
- [49] L.-A. Wu, M. Xiao, and H. J. Kimble, Squeezed states of light from an optical parametric oscillator, J. Opt. Soc. Am. B 4, 1465 (1987).
- [50] H. Vahlbruch, M. Mehmet, K. Danzmann, and R. Schnabel, Detection of 15 dB squeezed states of light and their application for the absolute calibration of photoelectric quantum efficiency, Phys. Rev. Lett. 117, 110801 (2016).
- [51] D. Stoler, Equivalence classes of minimum uncertainty packets, Phys. Rev. D 1, 3217 (1970).
- [52] D. Stoler, Equivalence classes of minimum-uncertainty packets. ii, Phys. Rev. D 4, 1925 (1971).
- [53] G. Agarwal, Nonclassical characteristics of the marginals for the radiation field, Opt. Commun. **95**, 109 (1993).
- [54] W. Vogel, Nonclassical states: An observable criterion, Phys. Rev. Lett. 84, 1849 (2000).
- [55] T. Richter and W. Vogel, Nonclassicality of quantum states: A hierarchy of observable conditions, Phys. Rev. Lett. 89, 283601 (2002).
- [56] L. Innocenti, L. Lachman, and R. Filip, Nonclassicality detection from few Fock-state probabilities, npj Quantum Inf. 8, 30 (2022).

- [57] N. Brunner, D. Cavalcanti, S. Pironio, V. Scarani, and S. Wehner, Bell nonlocality, Rev. Mod. Phys. 86, 419 (2014).
- [58] V. S. Kovtoniuk, I. S. Yeremenko, S. Ryl, W. Vogel, and A. A. Semenov, Nonclassical correlations of radiation in relation to Bell nonlocality, Phys. Rev. A 105, 063722 (2022).
- [59] B. S. Tsirelson, Some results and problems on quantum Bell-type inequalities, Hadronic J. Suppl. 8, 329 (1993).
- [60] S. Abramsky and A. Brandenburger, The sheaf-theoretic structure of non-locality and contextuality, New J. Phys. 13, 113036 (2011).
- [61] R. T. Rockafellar, Convex Analysis (Princeton University Press, 1970).
- [62] D. Hug and W. Weil, Lectures on Convex Geometry (Springer Cham, 2020).
- [63] P. L. Kelley and W. H. Kleiner, Theory of electromagnetic field measurement and photoelectron counting, Phys. Rev. 136, A316 (1964).
- [64] A. A. Semenov, J. Samelin, C. Boldt, M. Schünemann, C. Reiher, W. Vogel, and B. Hage, Photocounting measurements with dead time and afterpulses in the continuous-wave regime (2023), arXiv:2303.14246 [quantph].
- [65] V. A. Uzunova and A. A. Semenov, Photocounting statistics of superconducting nanowire single-photon detectors, Phys. Rev. A 105, 063716 (2022).
- [66] R. Filip and L. Lachman, Hierarchy of feasible nonclassicality criteria for sources of photons, Phys. Rev. A 88, 043827 (2013).
- [67] T. Frankel, The geometry of physics: an introduction, 3rd ed. (Cambridge University Press, 2012).
- [68] K. Banaszek, A. Dragan, K. Wódkiewicz, and C. Radzewicz, Direct measurement of optical quasidistribution functions: Multimode theory and homodyne tests of Bell's inequalities, Phys. Rev. A 66, 043803 (2002).
- [69] J. Farkas, Theorie der einfachen Ungleichungen, J. die Reine und Angew. Math. (Crelles Journal) 1902, 1 (1902).